Transfemoral limb loss modestly increases the metabolic cost of optimal control simulations of walking

Ross H. Miller[1,*], Elizabeth M. Bell[1,2], Elizabeth Russell Esposito[3]
[1]Department of Kinesiology, University of Maryland, College Park, MD, USA
[2]Department of Kinesiology, Towson University, Towson, MD, USA
[3]Military Operational Medicine Research Program, Fort Detrick, MD, USA
*Corresponding author: rosshm@umd.edu

ABSTRACT

Unlike the case of transtibial limb loss, high-functioning military service members with transfemoral limb loss have a high metabolic cost of walking compared to able-bodied peers. In transtibial limb loss, computer simulations suggest that the maintenance of muscle strength between pre- and post-limb loss can maintain the pre-limb loss metabolic cost. Here we performed optimal control simulations of walking with and without transfemoral limb loss to determine if transfemoral limb loss *per se* increases the metabolic cost of walking. OpenSim Moco was used to generate optimal control simulations of walking in 15 virtual subjects that minimized the weighted sum of (i) deviations from average able-bodied gait mechanics and (ii) the gross metabolic cost of walking, pre-limb loss in models with two intact biological limbs, and post-limb loss with one of the limbs replaced by a transfemoral prosthesis. No other changes were made to the model. Metabolic cost post-limb loss increased by 0.7-9.3% ($p < 0.01$) depending on whether cost was scaled by total body mass or biological body mass and on whether the prosthetic knee was passive or non-passive. The post-limb loss model had numerous features that predisposed it to low metabolic cost. These results suggest that transfemoral limb loss *per se* increases the metabolic cost of walking, but that the large differences above able-bodied peers of ~20-45% in most gait analysis experiments may be avoidable, even when minimizing deviations from able-bodied gait mechanics.

1. INTRODUCTION

Loss of a lower limb above the knee, i.e. transfemoral limb loss, is associated with a variety of deviations from the typical "able-bodied" mechanics and energetics of walking. Examples include hip-hiking and a relatively high metabolic cost (Carse et al., 2020). Gait deviations are thought to play a role in mobility, quality of life, and risk for secondary physical conditions in individuals with limb loss (Gailey et al., 2008). High energy expenditure of walking in older adults has been associated prospectively with slowing of walking speed (Schrack et al., 2016), hippocampus deterioration (Dougherty et al., 2022), and increasing perceived fatiguability (Schrack et al., 2020). Avoiding gait deviations and maintaining an economical gait are therefore important clinical goals following limb loss.

Military service members with transtibial limb loss do not have high metabolic costs of walking compared to age-matched able-bodied service members walking at similar speeds (Russell Esposito et al., 2014; Jarvis et al., 2017). The ability of these individuals to avoid high metabolic costs was speculatively attributed to their strength and fitness relative to the general limb loss population. This speculation was supported by optimal control simulations, where replacing one of a musculoskeletal model's lower limbs with a transtibial prosthesis did not increase the metabolic cost of walking with minimal gait deviations if the strength of the

remaining muscles was retained (Russell Esposito & Miller, 2018; Miller & Russell Esposito, 2021). Transtibial limb loss *per se* therefore did not increase the metabolic cost of walking. The assumption of no change in muscle strength following limb loss is of course not realistic, but it allows for isolation of the effect of the non-modifiable factor (loss of a limb) from modifiable factors like strength, within the limitations of the modeling assumptions. However, these findings are unique to transtibial limb loss. Relatively young service members with transfemoral limb loss still had a higher metabolic cost than able-bodied controls (Jarvis et al., 2017; Russell Esposito et al., 2018). Individuals with transtibial limb loss, transfemoral limb loss, and controls may have different relationships between metabolic cost and other gait sub-tasks such as lateral balance (Ijmker et al., 2014). It is therefore unclear if the finding that limb loss *per se* does not increase the metabolic cost of walking also pertains to transfemoral limb loss.

Therefore, the purpose of this study was to perform optimal control simulations of walking to isolate the effect of unilateral transfemoral limb loss on metabolic cost. Based on previous experiments on military service members (Jarvis et al., 2017; Russell Esposito et al., 2018), we expected that replacing one of a three-dimensional musculoskeletal model's limbs with a transfemoral prosthetic limb would increase the metabolic cost of walking when the model attempted to minimize a weighted summation of metabolic cost and deviations from able-bodied walking mechanics.

2. METHODS

2.1. Pre-Limb Loss Model Description

Simulations of walking were performed using a three-dimensional model of the human musculoskeletal system with 31 degrees of freedom and 120 Hill-based muscle models (Fig. 1). The model was a modified version of the model described by Rajagopal et al. (2016), implemented in version 4.4 of OpenSim software (Delp et al., 2007). The following modifications were made to the original model to accommodate use in gradient-based optimal control simulations with OpenSim Moco software (Dembia et al., 2020):

1. The muscles were changed to "DeGrooteFregly2016"-type muscles, which have dynamics suitable for gradient-based optimization (DeGroote et al., 2016).
2. Muscle parameters were adjusted as described by Lai et al. (2017) to include more realistic knee muscle moment arms at up to 140° of knee flexion. Although 140° of knee flexion is not typically necessary for walking with or without limb loss, this modification avoids biasing the optimization solution domain towards gaits with shallow flexion.
3. Torsional spring-dampers representing the passive stiffness of ligaments and other non-muscular joint structures were added to the joints (Anderson, 1999).
4. Eleven sphere-shaped Hunt-Crossley contact elements (Sherman et al., 2011) were added to the plantar surface of each foot (Fig. 1). The modulus (3.06 MPa) and damping coefficient (2.0 s/m) of the contact elements were set so that the heel contact sphere deformation and energy return were similar to the heel region of a human foot in an athletic shoe (Aerts & De Clercq, 1993). The frictional contact forces were a Stribeck function (Sherman et al., 2011) with respective static, dynamic, and viscous friction coefficients of 0.8, 0.8, and 0.5, and transition velocity 0.2 m/s.

The following additional modifications were not strictly necessary for Moco but were made for model fidelity:

1. Eight muscles actuating the lumbar joint (bilateral pairs of erector spinae, external obliques, internal obliques, rectus abdominus) and 12 muscles actuating each arm

(biceps, brachialis, long and short heads of the triceps, anterior, middle, and posterior deltoid, pectoralis, latissimus dorsi, supraspinatus, infraspinatus, subscapularis) were added. The muscle geometry and parameters were taken from several sources (Anderson & Pandy, 1999; Holzbaur et al., 2005; Raabe & Chaudhari, 2016).

2. Muscle-specific time constants for activation and deactivation were defined as functions of mass and fast-twitch fiber fraction (Winters & Stark, 1985). Muscle mass was the product of physiological cross-sectional area, optimal fiber length, and density (Umberger et al., 2003). Fast-twitch fiber fractions were referenced from Miller (2018).
3. The specific tension, which determines the muscle maximum isometric forces, was reduced to 40 N/cm^2 from its original value of 60 N/cm^2. With the original value, the model was able to produce unrealistically high maximum isometric ankle torques.
4. Eight smaller muscles included in the popular "gait2392" model but not in the original Rajagopal et al. (2016) were added: bilateral pairs of gemelli, pectineus, peroneus tertius, and quadratus femoris.

Muscle metabolic rates were calculated using a smoothed version of the Bhargava et al. (2004) energy model included in Moco. The non-muscular basal metabolic rate was calculated by assuming a default whole-body basal rate of 1.4 W per kg of whole-body mass, then subtracting the minimum muscle metabolic rates of 1.0 W per kg muscle mass. The whole-body metabolic rate was then the sum of the muscle metabolic rates and the non-muscular basal rate.

[Figure 1 here]

2.2. Post-Limb Loss Model Description

To model transfemoral limb loss, the 12 muscles spanning the right ankle joint were removed, and the muscles spanning the right knee joint had their attachment point moved proximally to locations 8 cm from the distal end of the femur. The muscle reattachments and corresponding shortening of tendon slack lengths emulated a typical myodesis surgery as described by Ranz et al. (2017), preserving as much of the original muscle tension in the neutral hip position as possible. The right knee, ankle, subtalar, and toe joints had linear torque-angle relationships representing the prosthetic joints:

$$\tau = -k(\theta - \theta_0) - b\dot{\theta} \qquad \text{(Eq. 1)}$$

where τ is the torque at the prosthetic joint, θ is the joint angle, k and b are prosthesis stiffness and damping parameters, and θ_0 is the neutral prosthetic joint position. The right patella was removed, the mass of the right femur was reduced by 20%, and the mass of the right shank and foot were reduced by 50%. The resulting total mass of the transfemoral prosthesis model was 3.5 kg. Jaegers et al. (1993) reported a range of 2.9-4.0 kg for devices used by 11 individuals with transfemoral limb loss.

Equation 1 is a simple but reasonably realistic phenomenological model of many unpowered prosthetic ankles/feet, and of "mechanically passive" prosthetic knees that have a constant joint stiffness. However, many prosthetic knee devices have mechanisms that effectively alter the stiffness of the prosthetic joint, e.g. switching between a high-stiffness mode during the stance phase of walking and a low-stiffness mode during the swing phase. Examples include popular microprocessor-controlled prosthetic knees (Kaufman et al., 2008). OpenSim includes a "ClutchedPathSpring" actuator that switches between zero and non-zero stiffnesses based on a time-varying control signal. However, we had difficulty getting optimizations in Moco to converge when using a ClutchedPathSpring actuator. We instead used a simpler

approach to model prosthetic knee phenomena more complex than Eq. 1 by adding an "ActivationCoordinateActuator" to the passive prosthetic knee model of Eq. 1:

$$\tau = -k(\theta - \theta_0) - b\dot{\theta} + \alpha\tau_{max} \quad \text{(Eq. 2)}$$

where $\alpha \in [-1,1]$ is the activation level and τ_{max} = 100 Nm is the maximum active prosthetic knee torque. The activation time constant was 100 ms. The prosthetic foot and ankle joints were still unpowered when using Eq. 2 at the knee.

The post-limb loss model was otherwise identical to the pre-limb loss model. For example, the maximum isometric forces of the 108 muscles of the post-limb loss model were unadjusted from their values in the pre-limb loss model. No degrees of freedom were modeled at the interface between the prosthesis and the residual limb. The post-limb loss model was therefore more similar to an osseointegrated prosthesis that attaches rigidly to the residual limb, rather than a traditional socket-based prosthesis.

2.3. Simulations

2.3.1. Subjects

The computational speed of modern optimal control methods allows for simulations of multiple subjects, producing datasets that can undergo formal statistical analysis and hypothesis testing similar to studies on human participants. As a computer simulation study, the subjects in the present study were instances of the model described in §2.1-2.2 with different model parameter values. The pre-limb loss model had a standing height of 1.70 m and body mass of 75.3 kg. Post-limb loss, the total body mass was 70.8 kg, with 67.3 kg of biological mass and 3.5 kg of prosthesis mass. This instance of the model was defined as "Subject 00". Additional subjects were generated using the OpenSim "Scale Model" tool to scale the Subject 00 pre-limb loss model to the height and mass of each of the 14 able-bodied control participants from Russell Esposito et al. (2018), all of whom were United States military service members (mean age 26 years, range 22-44 years). The dimensions of all axes of all body segments in the model were scaled linearly by the ratio of the target height to the Subject 00 height. The mass of each body segment was scaled linearly by the ratio of the target total body mass to the Subject 00 total body mass. The segment dimension scaling also adjusted the muscle optimal fiber lengths and tendon slack lengths. Muscle maximum isometric forces were then scaled linearly by the ratio of the target whole-body mass to the Subject 00 whole-body mass.

Including Subject 00 and the 14 subjects scaled to the heights and masses from Russell Esposito et al. (2018), there was a total of 15 subjects in the study. We emphasize that these subjects were not intended to represent any specific individuals, and did not represent an exhaustive sensitivity analysis of the model's parameter values. The element of subjects in the present study is better viewed as a limited sensitivity analysis, providing some confidence that any reported effects were due to the independent variable (limb loss) and generalize beyond the original model's specific parameter values. The sample of 15 subjects had a minimum detectable effect size of 0.68 in the paired directional *t*-test of the change in metabolic cost pre- vs. post-limb loss, using standard long-term error rates of 5% for false-positives and 20% for false-negatives. In the present data, this effect size equated to a minimum detectable change in metabolic cost of about 1%.

A single high-functioning human participant with unilateral transfemoral limb loss completed an instrumented gait analysis of walking at their preferred "normal and comfortable" walking speed of 1.30 m/s. Ground reaction forces were measured at 1000 Hz using piezeoresistive force platforms (Kistler) and marker-based motion capture was performed at 200

Hz using optical cameras (Vicon) and used to calculate joint and segment angles with standard six-degrees-of-freedom methods (Miller et al., 2014). Participation was approved by the University of Maryland institutional review board, protocol #1826662. The participant was male, 26 years old, height 1.90 m, mass 96.3 kg, and had undergone limb loss due to traumatic injury. The participant was Medicare K-level 4, used a microprocessor-controlled prosthetic knee, had unusually high levels of strength, fitness, and mobility with a transfemoral prosthesis, and frequently participated in various sports and weight training.

2.3.2. Overview

The models described §2.1-2.2 were used to simulate periodic strides of walking at average speed 1.45 m/s and stride duration 1.0 s, values reported by Miller et al. (2014) for healthy adults walking at a subjective "normal and comfortable" pace. The simulations were posed as optimal control problems, finding the time-varying muscle excitations and associated model states that minimized the weighted sum of (i) deviations from average able-bodied gait mechanics and (ii) the gross metabolic cost, in the form of the cost function J:

$$J = \int_0^T \left[\frac{1}{NT} \sum_{i=1}^{N} \left(\frac{x_i(t) - \mu_i(t)}{\sigma_i} \right)^2 + \frac{w_1}{m\Delta x} \left(\dot{E}_b + \dot{E}_m(t) \right) \right] dt \qquad \text{(Eq. 3)}$$

The first term on the righthand side of Eq. 3 is the "gait deviations tracking error": $x_i(t)$ is the value of model variable i at time t, $\mu_i(t)$ is the mean of the analogous variable from the experimental gait analysis data of Miller et al. (2014), and σ_i is the standard deviation between-subjects of the experimental variable, averaged over the gait cycle. The N = 37 variables included in the tracking error term were the six translations and rotations of the pelvis, the 25 joint angles, and the three components of the ground reaction force under each foot. The square root of this term gives the average tracking error of the simulation, averaged over all timesteps of all variables, in multiples of the standard deviation. For example, a tracking error of 0.5 means that the simulation's values for these 37 variables deviated from the average gait mechanics, defined by $\mu_i(t)$, by 0.5 standard deviations on average. For the motions of toe flexion, subtalar inversion, hip internal rotation, and the non-sagittal shoulder motions, we had low confidence in the accuracy of the experimental data, so we increased the value of σ_i to $3\sigma_i$ for these variables. This change in weighting allowed for better tracking of variables that can be measured with greater confidence in their accuracy, such as the sagittal joint motions and the ground reaction forces.

The second term on the righthand side of Eq. 3 is the metabolic cost: $\dot{E}_b$ is the non-muscular basal metabolic rate, $\dot{E}_m(t)$ is the sum of the muscle metabolic rates, m is the total body mass, and Δx is the horizontal displacement of the center of mass. The weighting constant w_1 defines the relative emphasis the optimizer places on reducing the tracking error vs. the metabolic cost, which are generally in opposition (smaller tracking errors have greater metabolic costs). Values of w_1 = 0.05 to 0.15 produced realistic metabolic costs of roughly 3-4 J/m/kg during model development with the Subject 00 pre-limb loss model, and a middle value of w_1 = 0.10 was chosen. The same value (w_1 = 0.10) was thereafter used in all simulations of all subjects, pre- and post-limb loss. We emphasize that the goal of these simulations was not to produce simulations that necessarily resemble the mechanics and energetics of actual humans walking with a transfemoral prosthesis. Rather, the goal was to define specific clinically relevant objectives (walk with minimum deviations from a target gait and minimum metabolic cost) whose presence and relative weighting were identical for the pre- and post-limb loss simulations,

such that differences between simulations could be confidently attributed to independent variable (limb loss) without a confounding effect of differences in the goals of the movement.

The optimal control problems were converted to nonlinear programming problems and solved using the direct collocation method in OpenSim Moco software (Dembia et al., 2020). The model's state and control variables were discretized with a Hermite-Simpson transcription scheme, with 101 nodal values per variable spaced evenly over the stride duration, i.e. one node every 1% of the gait cycle. Simulation results in model development were invariant to finer grids tested up to 201 nodes per stride, at which point the computational speed of the simulations became impractically slow. A full stride was simulated because the assumption of bilateral symmetry involved in simulating a single step (Anderson & Pandy, 2001) is not valid for asymmetric limb loss locomotion. The nodal state and control variable values were optimized to minimize the value of Eq. 3, subject to constraints of the skeletal equations of motion, muscle activation and contractile dynamics, and task constraints of kinematic periodicity and average speed. The IPOPT solver within Moco was used for optimization (Wächter & Biegler, 2006), with constraint tolerance 10^{-4} and solver tolerance 10^{-3}.

2.3.3. Validation simulations

It is not possible to directly validate the model's accuracy for predicting changes in metabolic cost after limb loss since it would require impractical longitudinal data on human metabolic cost pre- and post-limb loss. We therefore gauged the model's validity for predicting changes in metabolic cost with changes in lower limb mechanics that conceptually resemble limb loss. Previously, we demonstrated the model's validity for predicting changes in metabolic cost with changes in foot mass and ankle stiffness (Miller & Russell Esposito, 2021). Here we added evaluations of the predicted changes in metabolic cost with changes in thigh mass and knee stiffness.

Browning et al. (2007) measured net metabolic rate of walking at 1.25 m/s with either +4 or +8 kg of mass added to each thigh (total of +8 or +16 kg). The data were well fit by a simple linear regression where the net metabolic rate increased by an average of 0.075 W/kg per kilogram of added mass. We added the same masses to the thigh segments of the Subject 00 pre-limb loss model and performed simulations of walking at 1.25 m/s using the cost function and simulation approach described in §2.3.2. The model's net metabolic rate in these simulations increased by 0.077 W/kg per kilogram of added mass.

Lewek et al. (2012) used a commercial knee brace that unilaterally limited the knee to about 30° of flexion, and reported an average increase in net metabolic power of 17% when walking at 1.25 m/s compared to walking with unrestricted knee motion. We simulated knee bracing by adding a "CoordinateLimitForce" actuator to the right knee of the Subject 00 pre-limb loss model that made it essentially impossible for the model to flex its knee beyond 30°, and performed simulations of walking at 1.25 m/s using the cost function and simulation approach described in §2.3.2. We were unable to achieve the magnitudes of metabolic rates reported by Lewek et al. (2012). For example, their baseline "control" condition with the knee brace unlocked had an average metabolic rate of 3.8 W/kg, which is unusually high for walking at 1.25 m/s. The model's net metabolic rate at 1.25 m/s without the CoordinateLimitForce was 2.60 W/kg. The difference here was likely due to unmodeled aspects of the brace that affected the symmetry of the human participant's walking gaits even with the brace unlocked. However, the model's increase in metabolic rate with the CoordinateLimitForce on the right knee was +0.74

W/kg, which compares well to the increase in Lewek et al. (2012) of 0.66±0.60 W/kg with the brace locked vs. unlocked.

Changing lower limb mass and joint stiffness of an intact biological limb is of course not equivalent to walking with a prosthetic lower limb. However, reasonably accurate model-based predictions of these changes provides some confidence in using the model to predict changes in metabolic cost for conditions that cannot easily be validated directly with experiments.

2.3.4. Pre-limb loss simulations

Simulations with the pre-limb loss models described in §2.1 were performed using the direct collocation method described in §2.3.2. The same tracking targets $\mu_i(t)$ and σ_i were used in the cost function (Eq. 3) for all subjects. Each simulation was performed with three different initial guesses using simulation results from a previous similar study (Miller & Russell Esposito, 2021) and the result with the lowest cost function score was retained for analysis. When none of these initial guesses produced a result with a realistic metabolic cost, additional simulations with different initial guesses were performed until a result with a metabolic cost within two standard deviations of the mean from Das Gupta et al. (2019) was found.

2.3.5. Post-limb loss simulations

Simulations with the post-limb loss models described in §2.2 were performed identically to the pre-limb loss simulations, with the exception that the standard deviations for the prosthetic limb's knee, ankle, subtalar, and toe joints in Eq. 3 were increased to $10\sigma_i$, effectively reducing the weight on accurate tracking of these variables. The weight on these variables was reduced because the tracking targets $\mu_i(t)$ were biological joint motions and it was expected that the model could not track these motions well with prosthetic joints. Motions of these joints in unpowered prostheses also typically do not closely resemble biological joint motions (e.g. Kobayashi et al., 2020). To approximate the patient-specific selection and adjustment process typical done in prosthesis prescription, the k, b, and θ_0 prosthetic joint parameters in Eq. 1 were optimized along with the model states and controls in Moco for each subject's post-limb loss simulation to minimize the cost function. Stiffness k was bounded on [1, 100] Nm/rad for the knee and [10, 1000] Nm/rad for the ankle. Damping b was bounded on [1, 10] Nm•s/rad for both joints. Neutral joint position θ_0 was bounded on [-10, 10] degrees for both joints. The prosthetic subtalar and toe joints were set to k = 400 Nm/rad, b = 1.0 Nm•s/rad, and θ_0 = 0°.

Post-limb loss simulations were performed twice for each subject, once with the passive prosthesis in Eq. 1 and once with the prosthesis that included the ActivationCoordinateActuator at the knee, Eq. 2. As noted earlier, the purpose of this actuator was to allow small deviations from the torque profile of the fully passive prosthetic knee, not to simulate a fully powered motorized prosthetic knee. This purpose was achieved by minimizing the control signal of the actuator in the cost function:

$$J = \int_0^T \left[\frac{1}{NT} \sum_{i=1}^{N} \left(\frac{x_i(t) - \mu_i(t)}{\sigma_i} \right)^2 + \frac{w_1}{m\Delta x} \left(\dot{E}_b + \dot{E}_m(t) \right) + w_2 u^2(t) \right] dt \qquad \text{(Eq. 4)}$$

where $u(t) \in [0,1]$ is the prosthetic knee ActivationCoordinateActuator's control signal. The weighting on this signal was given a high value of w_2 = 100. Given the value of w_1 = 0.1 in combination with w_2 = 100, the cost of using the ActivationCoordinateActuator to produce the target biological knee torque waveform equated to a very high increase in metabolic cost of +47 J/m/kg. The cost of using the powered prosthesis to alter the knee torque produced by the

passive component of the prosthesis by an average of 1.0 Nm across the gait cycle equated to an increase in metabolic cost of +0.1 J/m/kg. The model with the ActivationCoordinateActuator (Eq. 4) will hereafter be referred to the "non-passive" prosthesis model.

2.3.6. Outcome variables and statistics

The main outcome variable of each simulation was the gross metabolic cost, defined as the metabolic energy expended per unit distance traveled by the model's center of mass, divided by the body mass (units = J/m/kg). Paired Student's *t*-tests were used to test the hypothesis that metabolic cost is greater post-limb loss vs. pre-limb loss, for both the passive and non-passive prosthesis models. The threshold for significance was $p = 0.05$, with Bonferroni adjustments for multiple comparisons.

Some studies on the limb loss population scale metabolic cost by the "total mass", which includes the mass of the prosthesis (e.g. Jarvis et al., 2017). Others scale metabolic cost by the "biological mass", excluding the mass of the prosthesis (e.g. Russell Esposito et al., 2018). Because the prosthesis mass is a substantial fraction of the total body mass for individuals with transfemoral limb loss, the statistical analysis above was performed on post-limb loss metabolic costs scaled by total mass, and again when scaled by biological mass. With two statistical comparisons to the pre-limb loss simulations with the different prosthesis models, and two comparisons with different mass scaling, the threshold for rejecting the null hypothesis was $p = 0.05/4 = 0.0125$.

3. RESULTS

3.1. Gait Mechanics

The pre-limb loss simulations deviated from the average able-bodied walking data of Miller et al. (2014) by 0.31 SD on average, with little variation in this tracking accuracy between subjects (range 0.30-0.32 SD). Average tracking errors in the post-limb loss simulations ranged from 0.41-0.47 SD and did not differ much between the passive and non-passive prosthesis simulations (0.43±0.01 SD vs. 0.42±0.01 SD). Figures 2-5 show a typical tracking result, from the baseline model (Subject 00), for the pre- and post-limb loss simulations, using the passive prosthesis model in the post-limb loss case. Although the post-limb loss simulations did not attempt to track experimental gait data from human participants with limb loss, they still exhibited numerous prevalent gait deviations seen in individuals with unilateral transfemoral limb loss and passive prostheses (Table 1). The magnitudes of these deviations were assessed in the high-functioning human participant with transfemoral limb loss and were generally similar to the post-limb loss simulations, with the exception that the human participant did not have a substantial deviation in their torso lateral bending range of motion (Table 1).

The post-limb loss simulations did not exhibit notable vaulting, hitching, or hip circumduction to swing the prosthetic limb, although these deviations were reported in only 20-54% of participants in Carse et al. (2020) and were also not observed in substantial magnitudes in the high-functioning human participant.

[Table 1 here]

[Figures 2-5 here]

3.2. Metabolic Cost

Gross metabolic cost in the pre-limb loss simulations was 3.22±0.04 J/m/kg (mean±SD). In human participants, average metabolic cost of walking at typical, comfortable speeds ranges from about 3.0-3.7 J/m/kg in young, unimpaired adults in most studies (Das Gupta et al., 2019). the post-limb loss simulations with scaling by biological mass had metabolic costs of 3.42±0.05 J/m/kg. In comparison, the human participant with transfemoral limb loss and a microprocessor-controlled prosthesis had a metabolic cost of 3.56 J/m/kg when scaled by biological mass.

Metabolic costs for all simulations of all virtual subjects are shown in Fig. 6. In the post-limb loss simulations, metabolic cost was always significantly greater than the pre-limb loss metabolic cost, for all four cases tested: passive and non-passive prosthesis, scaling by total mass and by biological mass (all $p < 0.01$). Metabolic cost increased above the pre-limb loss simulations by an average of +0.7% ($p = 0.0099$) when using the non-passive prosthesis with scaling by total mass, by +3.9% ($p = 0.0013$) when using the passive prosthesis with scaling by total mass, by +6.0% ($p = 3.4 \cdot 10^{-12}$) when using the non-passive prosthesis with scaling by biological mass and by +9.3% ($p = 4.4 \cdot 10^{-7}$) when using the passive prosthesis with scaling by biological mass.

[Figure 6 here]

4. DISCUSSION

The purpose of this study was to determine if transfemoral limb loss increases metabolic cost of walking in optimal control simulations. The main finding was that converting one of the model's limbs to a transfemoral prosthesis increased the metabolic cost of walking with minimum gait deviations, regardless of whether the prosthesis was passive or non-passive, and regardless of whether the metabolic cost was scaled by biological body mass or total body mass. The limb loss model had several advantages predisposing it to low metabolic costs: it had a long residual limb, rigid limb-prosthesis interface, and high level of muscle strength, and could optimize its prosthetic stiffnesses, all of which have been associated with low metabolic cost (Boonstra et all, 1994; Kooiman et al., 2023; Nolan, 2012; Fey et al., 2012). The present results therefore suggest that unlike transtibial limb loss (Miller & Russell Esposito, 2021), transfemoral limb loss necessarily increases the metabolic cost of walking.

The main limitation of the present study is its modeling and simulation nature. While the post-limb loss simulations exhibited many of the gait deviations commonly seen in individuals with transfemoral limb loss (Table 1), we emphasize that the goal of these simulations was not to replicate reality in-silico or to emulate the gaits of any particular individuals. Rather, the goal was to isolate the effect of limb loss in and of itself on metabolic cost. In experiments on human participants, testing of this effect is confounded by other variables that tend to be affected by limb loss and can independently affect the metabolic cost of walking, such as changes in walking speed or other stride parameters, changes in muscle strength or other dimensions of fitness, and changes in sub-task priorities of walking. Computer modeling and simulation therefore allows for conclusions on the effect of transfemoral limb loss *per se*, independent of these confounders, within the limitations of modeling assumptions involved.

Relatedly, the increases in metabolic cost reported in these simulations of about 1-9% vs. the pre-limb loss case are much smaller than differences reported in experiments comparing human participants with and without transfemoral limb loss. In the most directly relevant comparison to the present simulations are studies on the military limb loss population, who compared to the general limb loss population are relatively young, strong, and fit, and often have

access to more extensive rehabilitation and prosthetics prescription programs with higher-functioning goals such as return-to-service. Metabolic cost in young military service members with transfemoral limb loss was on average 45% greater than age-matched able-bodied service members when scaled by biological body mass (Russell Esposito et al., 2018), and 20% greater when scaled by total body mass (Jarvis et al., 2017). We speculate that this difference between simulations and human experiments, which contrasts with findings in these same studies and our previous simulations on transtibial limb loss (Miller & Russell Esposito, 2021), is because the assumption in the simulations of maintenance of muscle strength between the pre- and post-limb loss conditions is less realistic for transfemoral limb loss than for transtibial limb loss. An optimistic interpretation of this difference between the present simulations and previous experiments is that while transfemoral limb loss may invariably increase the metabolic cost of walking, this increase does not necessarily need to be large and can be reduced by modifiable factors of strength and fitness. Nolan (2012) reported that a 10-week program of 20 strength-training sessions of the prosthetic-side hip muscles reduced the oxygen consumption rate of walking at 1.0 m/s by an average of 7%, and enabled treadmill running when the participants with transfemoral limb loss all reported inability to run pre-training.

A related point of comparison and what may be achievable through modifiable factors post-limb loss is the single human participant in the present study. This individual was included because they are unusually fit and mobile even compared to other high-functioning individuals with transfemoral limb loss. As an example of this individual's very high level of function, they were able to hop vertically on their prosthetic limb, which requires remarkable levels of prosthetic-side strength, balance, and confidence. This individual's metabolic cost of walking was only slightly above the range of costs in the post-limb loss simulations (Fig. 6), suggesting that the simulation result reported here of a small increase in metabolic cost post-limb loss may also be achievable in human participants. This suggestion is cautioned by the acknowledgement that this individual had a very long residual limb, but prior results are mixed on whether residual limb length has an appreciable effect on metabolic cost of walking (Boonstra et al., 1994; Bell et al., 2014).

As noted earlier, the post-limb loss simulations did not explicitly attempt to track gait mechanics data from individuals with limb loss, but nonetheless exhibited many of the common gait deviations associated with transfemoral limb loss (Table 1). This result suggests that these deviations may be unavoidable, at least qualitatively, in walking with transfemoral limb loss, at least when combined with the goal of a relatively low metabolic cost. Attempting to further suppress these deviations, i.e. track the able-bodied experimental data more closely, would be expected to increase metabolic cost. Previous simulations and experiments on human participants have also suggested that altering the gait mechanics to be more symmetric in individuals with unilateral lower limb loss comes with substantial increases in metabolic cost (Handford & Srinivasan, 2016; Wedge et al., 2022). A Pareto front between the two cost function terms in these simulations, gait deviations and metabolic cost, including conditions of direct tracking of gait mechanics from individuals with transfemoral limb loss, would be a useful direction for future work to elaborate on the relationship between gait deviations and metabolic cost.

The simulations with the non-passive prosthesis model (Eq. 2) had lower metabolic cost than simulations with the passive prosthesis model (Eq. 1), by an average of -2.9% regardless of the method of body mass scaling (Fig. 6). We emphasize that the non-passive prosthesis model was not intended to emulate fully-powered, motorized, robotic, etc. prosthetic knees. Rather, the

high weight placed on the prosthetic knee's excitation control (parameter w_2 in Eq. 4) allowed the knee to deviate only slightly from a fully-passive joint moment profile without increasing metabolic cost or gait deviations, and was included among the conditions tested here to determine of the results depended critically on the simple prosthetic knee model assumed in Eq. 1. Popular battery-powered, microprocessor-controlled knees generally function differently than Eqs. 2 and 4 in that they modulate the level of damping in the joint based on feedback signals, but they achieve a conceptually similar effect to Eqs. 2 and 4 in that a small amount of power is used to deviate slightly from a fully-passive knee moment profile. Kaufman et al. (2008) reported an average decrease in oxygen cost of walking of -2.3% when using microprocessor-controlled vs. passive mechanical prosthetic knees after an average of 18 weeks of acclimation, although this difference was not statistically significant. Most other conceptually similar studies have reported similar results (Wong et al., 2012). Powered prostheses that more closely emulate able-bodied knee mechanics, or that restore ground contact sensation, have achieved larger reductions in metabolic cost of walking in case studies (Martinez-Villalpando et al., 2011; Petrini et al., 2019).

The choice of scaling by biological body mass vs. total body mass affected metabolic cost by roughly 5% (Fig. 6), which can feasibly affect conclusions since the minimum detectable difference using modern pulmonary gas measurements is roughly 2% (Davidson et al., 2016; Guidetti et al., 2018). For example, the +0.7% change in metabolic cost scaled by total mass with the non-passive prosthesis, while statistically significant, is not reliably detectable in human experiments even if it is deemed meaningful, while the change of +6.0% in this same condition when scaling by biological mass is easily detectable. We suggest that scaling by biological body mass casts metabolic cost as an index of efficiency (energy expended per unit mass consuming that energy), while scaling by total body mass is more appropriate as an index of economy (energy expended per unit mass transported). The option of no scaling is appropriate when absolute energy expenditure is of interest. Regardless, the scaling choice should be clearly reported and the sensitivity of conclusions to this choice should be considered.

A final point of a technical nature may also have relevance to the challenge of walking with a transfemoral prosthesis. Compared to our previous study that used a similar model to simulate walking with a transtibial prosthesis (Miller & Russell Esposito, 2021), the present simulations with a transfemoral prosthesis were much more difficult optimization problems for the Moco/IPOPT software, requiring on average twice as many different initial guesses than the previous study to converge on a high-quality simulation result for each subject: good tracking similar to Figs. 2-5, realistically low metabolic costs seen in Fig. 6. The simulation results from other initial guesses not shown here tended to have very poor tracking of the target experimental data and/or unrealistically high metabolic costs on the order of 10 J/m/kg. One subject did not converge on the result in Fig. 6 until the 14th initial guess. If we accept the optimization process as a crude analog of goal-oriented human motor learning, this difficulty suggests that even if an individual has the physical capacity to walk with small gait deviations and low metabolic cost following transfemoral limb loss, achieving this gait in practice may be a long and difficult process.

Some additional limitations are worth highlighting to aid readers in gauging their confidence in the present results before concluding. First, with the high-dimensional solution domain and numerical method used in the optimizations, we cannot guarantee that all the simulations are near their global minimum in their solution domain. It is possible that post-limb loss simulations with lower metabolic costs than those shown in Fig. 6 exist, which could

feasibly change conclusions reached. We performed all simulations of all subjects with at least three different initial guesses and in some cases as many as 14 initial guesses in attempting the minimize the impact of this limitation. We also checked on the sensitivity of the results to the five results in Fig. 6 that were above the mean for the post-limb loss passive prosthesis condition, and the statistical outcome of a significantly greater metabolic cost post-limb loss was robust to their exclusion. Second, while we presented data gauging the model's ability to predict small changes in metabolic cost, its ability to predict pre- vs. post-limb loss changes in metabolic cost has not been validated, as there are no data in the literature to base this validation on. There are longitudinal data on changes in metabolic cost with osseointegrated vs. socket-based transfemoral prostheses (Van de Meent et al., 2013; Kooiman et al., 2023), which would be a useful addition to the present model's validity. Third, to our knowledge this is the first study to perform these types of simulations with a model of a prosthetic knee. Options for modeling a prosthetic knee in the current OpenSim/Moco software were limited, and the prosthetic knee models used here (Eqs. 1 and 2) were rather simple. Prosthetic knee design characteristics have overall had small and inconsistent effects on metabolic cost (Wong et al., 2012; Sawers & Hafner, 2013), so we do not think the simplicity of the knees modeled here is a major limitation. For example, preliminary tests in model development of polycentric- vs. single-axis knee rotation centers did not affect metabolic cost of the post-limb loss simulation.

In conclusion, replacing a biological limb of a three-dimensional full-body musculoskeletal model with a transfemoral prosthetic limb increase the metabolic cost of walking with minimal gait deviations, and induced many of the gait deviations commonly seen in human participants walking with transfemoral prostheses, even without any post-limb loss changes in muscle strength. However, the magnitude of the increase in metabolic cost was considerably smaller than differences in metabolic cost typically seen in human participants with transfemoral limb loss vs. able-bodied participants, particularly when a small amount of power was delivered to the prosthetic knee. These results suggest that a large increase in metabolic cost post-transfemoral limb loss may be avoidable in the long-term by maintenance of muscle strength and prosthetic knee technology.

DATA AVAILABILITY

The data and models for these simulations are available at: https://simtk.org/projects/umocod

ACKNOWLEDGMENTS

This study was supported by funding from the Army Advanced Medical Technology Initiative, administered to the University of Maryland via Madigan Army Medical Center. There was no additional external funding received for this study. The funders had no role in study design, data collection and analysis, decision to publish, or preparation of the manuscript.

REFERENCES

Aerts P, De Clercq D (1993). Deformation characteristics of the heel region of the shod foot during a simulated heel strike: the effect of varying midsole hardness. *Journal of Sports Sciences* **11**, pp. 449-461; doi: 10.1080/02640419308730011

Anderson FC (1999). A dynamic optimization solution for a complete cycle of normal gait. Doctoral dissertation, University of Texas at Austin; doi: none assigned

Anderson FC, Pandy MG (1999). A dynamic optimization solution for vertical jumping in three dimensions. *Computer Methods in Biomechanics & Biomedical Engineering* **2**, pp. 201-231; doi: 10.1080/10255849908907988

Anderson FC, Pandy MG (2001). Dynamic optimization of human walking. *Journal of Biomechanical Engineering* **123**, pp. 381-390; doi: 10.1115/1.1392310

Bell JC, Wolf EJ, Schnall BL, Tis JE, Potter BJ (2014). Transfemoral amputations: is there an effect of residual limb length and orientation on energy expenditure? *Clinical Orthopaedics & Related Research* **472**, pp. 3055-3061; doi: 10.1007/s11999-014-3630-x

Boonstra AM, Schrama J, Fidler V, Eisma WH (1994). The gait of unilateral transfemoral amputees. *Scandinavian Journal of Rehabilitation Medicine* **23**, pp. 217-223; doi: none assigned

Bhargava LJ, Pandy MG, Anderson FC (2004). A phenomenological model for estimating metabolic energy consumption in muscle contraction. *Journal of Biomechanics* **37**, pp. 81-88; doi: 10.1016/S0021-9290(03)00239-2

Browning RC, Modica JR, Kram R, Goswami A (2007). The effects of adding mass to the legs on the energetics and biomechanics of walking. *Medicine & Science in Sports & Exercise* **39**, pp. 515-525; doi: 10.1249/mss.0b013e31802b3562

Carse B, Scott H, Brady L, Colvin J (2020). A characterisation of established unilateral transfemoral amputee gait using 3D kinematics, kinetics and oxygen consumption measures. *Gait & Posture* **75**, pp. 98-104; doi: 10.1016/j.gaitpost.2019.09.029

Das Gupta S, Bobbert MF, Kistemaker DA (2019). The metabolic cost of walking in healthy young and older adults: a systematic review and meta analysis. *Scientific Reports* **9**, article 9956; doi: 10.1038/s41598-019-45602-4

Davidson A, Gardinier ES, Gates DH (2016). Within and between-day reliability of energetic cost measures during treadmill walking. *Cogent Engineering* **3**, article 1251028.

De Groote F, Kinney AL, Rao AV, Fregly BJ (2016). Evaluation of direct collocation optimal control problem formulations for solving the muscle redundancy problem. *Annals of Biomedical Engineering* **44**, pp. 2922-2936; doi: 10.1007/s10439-016-1591-9

Delp SL, Anderson FC, Arnold AS, Loan P, Habib A, John CT, Guendelman E, Thelen DG (2007). OpenSim: open-source software to create and analyze dynamic simulations of movement. *IEEE Transactions on Biomedical Engineering* **54**, pp. 1940-1950; doi: 10.1109/TBME.2007.901024

Dembia CL, Bianco NA, Falisse A, Hicks JL, Delp SL (2020). OpenSim Moco: Musculoskeletal optimal control. *PLoS Computational Biology* **16**, article e1008493; doi: doi.org/10.1371/journal.pcbi.1008493

Dougherty RJ, Liu F, An Y, Wanigatunga AA, Tian Q, Davatzikos C, Simonsick EM, Ferrucci L, Resnick SM, Schrack JA (2022). Energetic cost of walking and brain atrophy in mid-to-late life. *Journals of Gerontology: Medical Sciences* **77**, pp. 2068-2076; doi: 10.1093/gerona/glab309

Fey NP, Klute GK, Neptune RR (2012). Optimization of prosthetic foot stiffness to reduce metabolic cost and intact knee loading during below-knee amputee walking: a theoretical study. *Journal of Biomechanical Engineering* **134**, article 111005; doi: 10.1115/1.4007824

Gailey R, Allen K, Castles J, Kucharik J, Roeder M (2008). Review of secondary physical conditions associated with lower-limb amputation and long-term prosthesis use. *Journal of Rehabilitation Research & Development* **45**, pp. 15-30; doi: 10.1682/JRRD.2006.11.0147

Guidetti L, Meucci M, Bolletta F, Emerenziani GP, Gallotta MC, Baldari C (2018). Validity, reliability and minimum detectable change of COSMED K5 portable gas exchange system in breath-by-breath mode. *PLoS One* **13**, article e0209925; doi: doi.org/10.1371/journal.pone.0209925

Handford ML, Srinivasan M (2016). Robotic lower limb prosthesis design through simultaneous computer optimizations of human and prosthesis costs. *Scientific Reports* **6**, article 19983; doi: 10.1038/srep19983

Holzbaur KRS, Murray WM, Delp SL (2005). A model of the upper extremity for simulating musculoskeletal surgery and analyzing neuromuscular control. *Annals of Biomedical Engineering* **33**, pp. 829-840; doi: 10.1007/s10439-005-3320-7

Ijmker T, Noten S, Lamoth CJ, Beek PJ, van der Woude LHV, Houdijk H (2014). Can external lateral stabilization reduce the energy cost of walking in persons with a lower limb amputation? *Gait & Posture* **40**, pp. 616-621; doi: 10.1016/j.gaitpost.2014.07.013

Jaegers SMHJ, Vos LDW, Rispens P, Hof AL (1993). The relationship between comfortable and most metabolically efficient walking speed in persons with unilateral above-knee amputation. *Archives of Physical Medicine & Rehabilitation* **74**, pp. 521-525; doi: 10.1016/0003-9993(93)90117-S

Jarvis HL, Bennett AN, Twiste M, Phillip RD, Etherington J, Baker R (2017). Temporal spatial and metabolic measures of walking in highly functional individuals with lower limb amputations. *Archives of Physical Medicine & Rehabilitation* **98**, pp. 1389-1399; doi: 10.1016/j.apmr.2016.09.134

Kaufman KR, Levine JA, Brey RH, McCrady SK, Badgett DJ, Joyner MJ (2008). Energy expenditure and activity of transfemoral amputees using mechanical and microprocessor-controlled prosthetic knees. *Archives of Physical Medicine & Rehabilitation* **89**, pp. 1380-1385; doi: 10.1016/j.apmr.2007.11.053

Kobayashi T, Hisano G, Namiki Y, Hashizume S, Hobara H (2020). Walking characteristics of runners with a transfemoral or knee-disarticulation prosthesis. *Clinical Biomechanics* **80**, article 105132; doi: 10.1016/j.clinbiomech.2020.105132

Kooiman V, Hakat L, Verdonschot N, Leijendekkers R, Weerdesteyn V (2023). Oxygen consumption and gait dynamics in transfemoral bone-anchored prosthesis users compared to socket-prosthesis users: a cross-sectional study. *Gait & Posture* **103**, pp. 12-18; doi: 10.1016/j.gaitpost.2023.04.008

Lai AKM, Arnold AS, Wakeling JM (2017). Why are antagonist muscles co-activated in my simulation? A musculoskeletal model for analysing human locomotor tasks. *Annals of Biomedical Engineering* **45**, pp. 2762-2774; doi: 10.1007/s10439-017-1920-7

Lewek MD, Osborn AJ, Wutzke CJ (2012). The influence of mechanically and physiologically imposed stiff-knee gait patterns on the energy cost of walking. *Archives of Physical Medicine & Rehabilitation* **93**, pp. 123-128; doi: 10.1016/j.apmr.2011.08.019

Martinez-Villalpando E, Mooney L, Elliott G, Herr H (2011). Antagonistic active knee prosthesis: a metabolic cost of walking comparison with a variable-damping prosthetic knee. *Proceedings of the 33rd Annual Meeting of the IEEE Engineering in Medicine & Biology Society*, pp. 8519-8522; doi: 10.1109/IEMBS.2011.6092102

Miller RH (2018). Hill-based muscle modeling. In: Müller B, Wolf SI (eds.), *Handbook of Human Motion*, pp. 373-493. Berlin: Springer; doi: 10.1007/978-3-319-14418-4_203

Miller RH, Edwards WB, Brandon SCE, Morton AM, Deluzio KJ (2014). Why don't most runners get knee osteoarthritis? A case for per-unit-distance loads. *Medicine & Science in Sports & Exercise* **46**, pp. 572-579; doi: 10.1249/mss.0000000000000135

Miller RH, Russell Esposito E (2021). Transtibial limb loss does not increase metabolic cost in three-dimensional computer simulations of human walking. *PeerJ* **9**, article e11960; doi: 10.7717/peerj.11960

Nolan L (2012). A training programme to improve hip strength in persons with lower limb amputation. *Journal of Rehabilitation Medicine* **44**, pp. 241-248; doi: 10.2340/16501977-0921

Petrini FM, Bumbasirevic M, Valle G, Ilic V, Mijović P, Čvančara P, Barberi F, Katic N, Bortolotti D, Andreu D, Lechler K, Lesic A, Mazic S, Mijović B, Guiraud D, Stieglitz T, Alexandersson A, Micera S, Raspopovic S (2019). Sensory feedback restoration in leg amputees improves walking speed, metabolic cost and phantom pain. *Nature Medicine* **25**, pp. 1356-1363; doi: 10.1038/s41591-019-0567-3

Raabe ME, Chaudhari AMW (2016). An investigation of jogging biomechanics using the full-body lumbar spine model: model development and validation. *Journal of Biomechanics* **49**, pp. 1238-1243; doi: 10.1016/j.jbiomech.2016.02.046

Rajagopal A, Dembia CL, DeMers MS, Delp DD, Hicks JL, Delp SL (2016). Full-body musculoskeletal model for muscle-driven simulation of human gait. *IEEE Transactions on Biomedical Engineering* **63**, pp. 2068-2079; doi: 10.1109/TBME.2016.2586891

Ranz EC, Wilken JM, Gajewski DA, Neptune RR (2017). The influence of limb alignment and transfemoral amputation technique on muscle capacity during gait. *Computer Methods in Biomechanics & Biomedical Engineering* **20**, pp. 1167-1174; doi: 10.1080/10255842.2017.1340461

Russell Esposito E, Rodriguez KM, Ràbago CA, Wilken JM (2014). Does unilateral transtibial amputation lead to greater metabolic demand during walking? *Journal of Rehabilitation Research & Development* **51**, pp. 1287-1296; doi: 10.1682/JRRD.2014.06.0141

Russell Esposito E, Ràbago CA, Wilken JM (2018). The influence of traumatic transfemoral amputation on metabolic cost across walking speeds. *Prosthetics & Orthotics International* **42**, pp. 214-222; doi: 10.1177/0309364617708649

Russell Esposito E, Miller RH (2018). Maintenance of muscle strength retains a normal metabolic cost in simulated walking after transtibial limb loss. *PLoS One* **13**, article e0191310; doi: 10.1371/journal.pone.0191310

Sawers AB, Hafner BJ (2013). Outcomes associated with the use of microprocessor-controlled prosthetic knees among individuals with unilateral transfemoral limb loss: a systematic review. *Journal of Rehabilitation Research & Development* **50**, pp. 273-314; doi: 10.1682/JRRD.2011.10.0187

Schrack JA, Zipunnikov V, Simonsick EM, Studenski S, Ferrucci L (2016). Rising energetic cost of walking predicts gait speed decline with aging. *Journals of Gerontology: Medical Sciences* **71**, pp. 947-953; doi: 10.1093/gerona/glw002

Schrack JA, Wanigatunga AA, Zipunnikov V, Kuo PL, Simonsick EM, Ferrucci L (2020). Longitudinal association between energy regulation and fatigability in mid-to-late life. *Journals of Gerontology: Medical Sciences* **75**, pp. e74-e80; doi: 10.1093/gerona/glaa011

Sherman MA, Seth A, Delp SL (2011). Simbody: multibody dynamics for biomedical research. *Procedia IUTAM* **2**, pp. 241-261; doi: 10.1016/j.piutam.2011.04.023

Umberger BR , Gerritsen KGM, Martin PE (2003). A model of human muscle energy expenditure. *Computer Methods in Biomechanics & Biomedical Engineering* **6**, pp. 99-111; doi: 10.1080/1025584031000091678

Van de Meent H, Hopman MT, Frölke JP (2013). Walking ability and quality of life in subjects with transfemoral amputation: a comparison of osseointegration with socket prostheses. *Archives of Physical Medicine & Rehabilitation* **94**, pp. 2174-2178; doi: 10.1016/j.apmr.2013.05.020

Wächter A, Biegler LT (2006). On the implementation of an interior-point filter line-search algorithm for large-scale nonlinear programming. *Mathematical Programming* **106**, pp. 25-57; doi: 10.1007/s10107-004-0559-y

Wedge RD, Sup FC, Umberger BR (2022). Metabolic cost of transport and stance time asymmetry in individuals with unilateral transtibial amputation using a passive prostheses while walking. *Clinical Biomechanics* **94**, article 105632; doi: 10.1016/j.clinbiomech.2022.105632

Winters JM, Stark L (1985). Analysis of fundamental human movement patterns through the use of in-depth antagonistic muscle models. *IEEE Transactions on Biomedical Engineering* **32**, pp. 826-839; doi: 10.1109/TBME.1985.325498

Wong CK, Benoy S, Blackwell W, Jones S, Rahal R (2012). A comparison of energy expenditure in people with transfemoral amputation using microprocessor and nonmicroprocessor knee prostheses: a systematic review. *Journal of Prosthetics & Orthotics* **24**, pp. 202-208; doi: 10.1097/JPO.0b013e31826f5e51

Table 1: Gait deviations commonly seen in human participants with transfemoral limb loss that had magnitudes of at least 3° (kinematics) or at least 3% bodyweight (kinetics) in the post-limb loss simulations when using the passive prosthesis. "Lesser" and "greater" refers to differences in comparison to the able-bodied pre-limb loss simulation. "Asymmetric" refers to the post-limb loss prosthetic limb vs. the intact limb. The "Prevalence" column is the fraction of 60 participants with unilateral transfemoral limb loss who exhibited these deviations in Carse et al. (2020). In the "Magnitude" columns, data labeled "Simulation" compare the post-limb loss vs. pre-limb loss simulations, or the post-limb loss prosthetic limb vs. intact limb, depending on the deviation in question. Data labeled "Human" compare the high-function human participant with transfemoral limb loss either to the referenced able-bodied human experimental means (Miller et al., 2014) or between their prosthetic vs. intact limb, depending on the deviation in question.

	Magnitude		
Deviation	**Simulation**	**Human**	**Prevalence**
Lesser anterior ground reaction force peak on prosthetic side	4.9 %BW	10.6 %BW	100%
Lesser posterior ground reaction force peak on prosthetic side	5.3 %BW	4.1 %BW	95%
Asymmetric late-stance vertical ground reaction force peaks	12.1 %BW	15.8 %BW	81%
Lesser early-stance knee flexion peak on prosthetic side	9.8°	11.7°	98%
Lesser late-stance hip extension peak on prosthetic side	6.3°	7.6°	82%
Greater average anterior pelvic tilt	3.1°	9.8°	77%
Greater torso lateral bending range of motion	5.9°	0.6°	92%

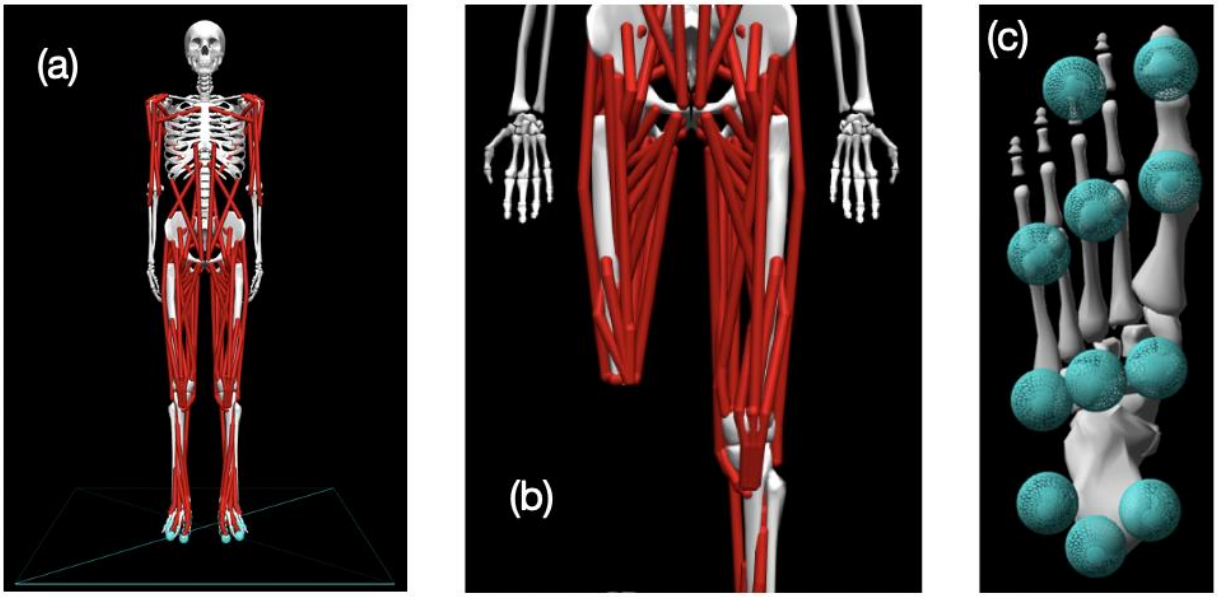

Figure 1: (a) Pre-limb loss version of the OpenSim model; (b) The model modified to include transfemoral limb loss at the right thigh; (c) Plantar surface of the model's foot with contact spheres.

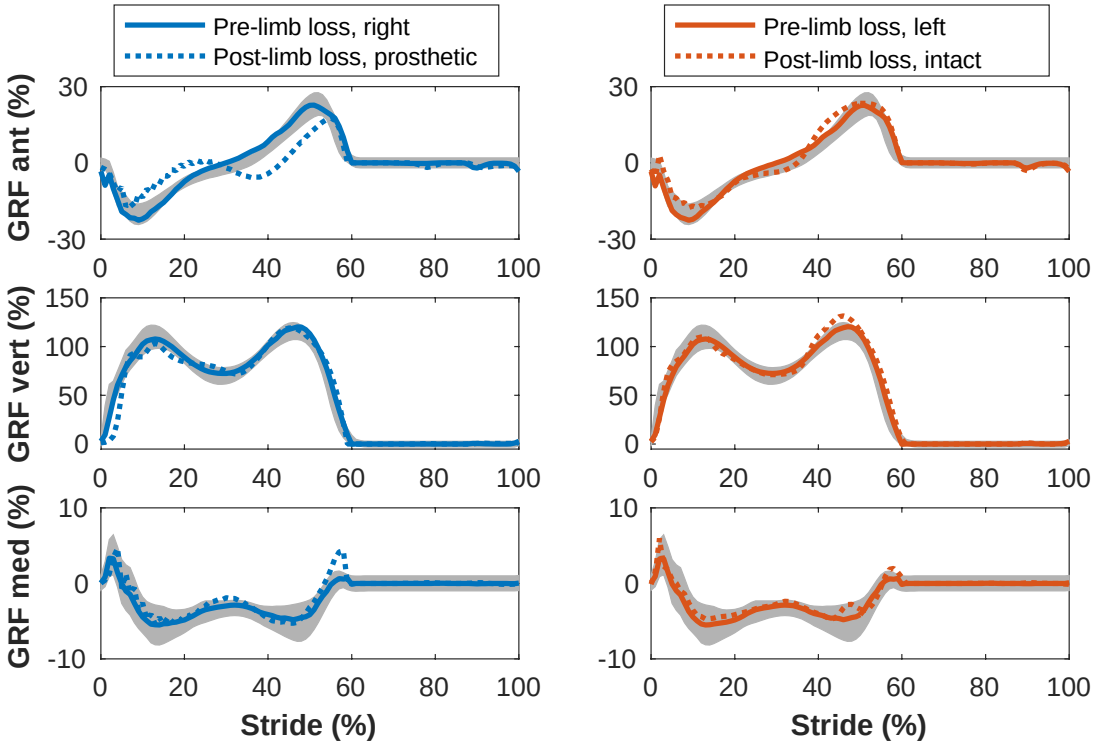

Figure 2: Ground reaction forces (GRF) in the anterior, vertical, and medial directions during the stride cycle for the pre-limb loss (solid lines) and post-limb loss (broken lines) simulations. Data begin and end at heel-strike of the leg indicated in the legends heading each column. Shaded areas are one standard deviation around mean human experimental walking data (Miller et al., 2014).

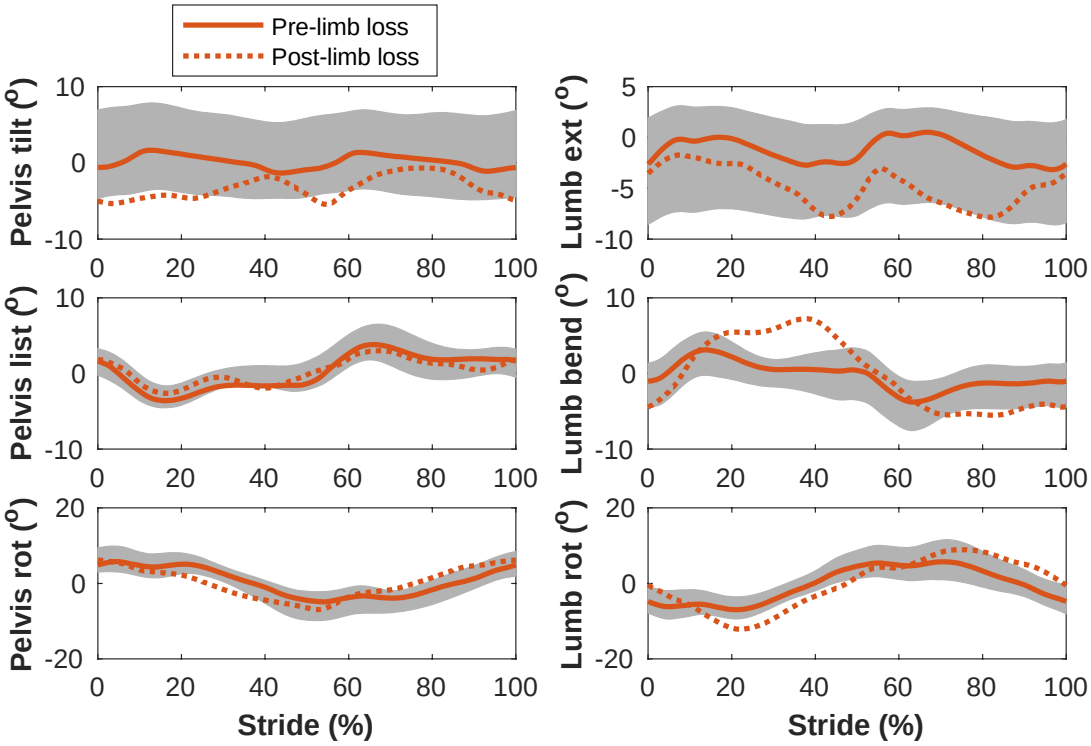

Figure 3: Pelvis and lumbar angles during the stride cycle for the pre-limb loss (solid lines) and post-limb loss (broken lines) simulations. Data begin and end at heel-strike of the right leg, which was the prosthetic leg post-limb loss. Shaded areas are one standard deviation around mean human experimental walking data (Miller et al., 2014).

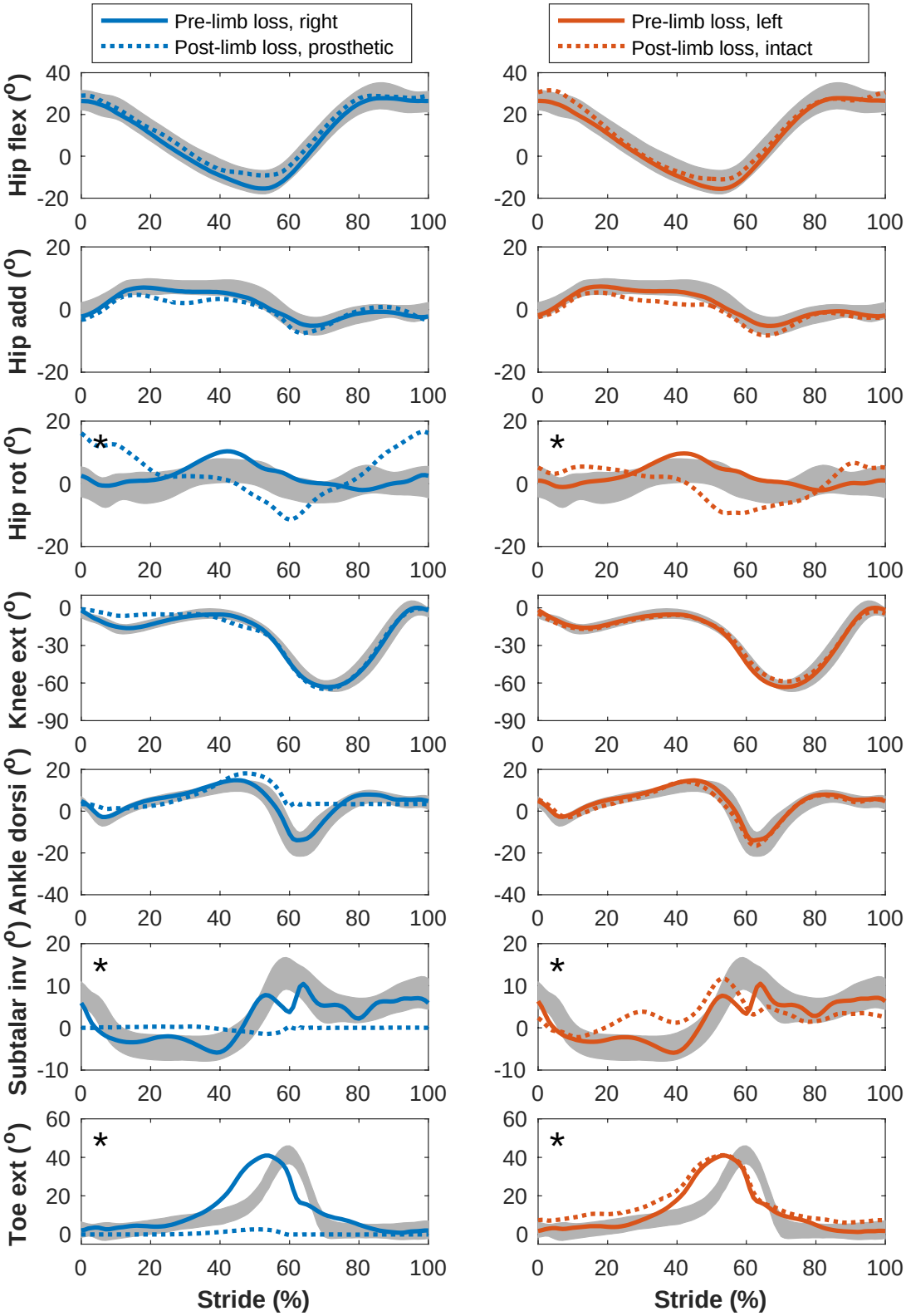

Figure 4: Lower limb joint angles during the stride cycle for the pre-limb loss (solid lines) and post-limb loss (broken lines) simulations. Data begin and end at heel-strike of the leg indicated in the column headings. Shaded areas are one standard deviation around mean human experimental walking data (Miller et al., 2014). Panels marked with * were variables with reduced tracking weight in the simulation cost function.

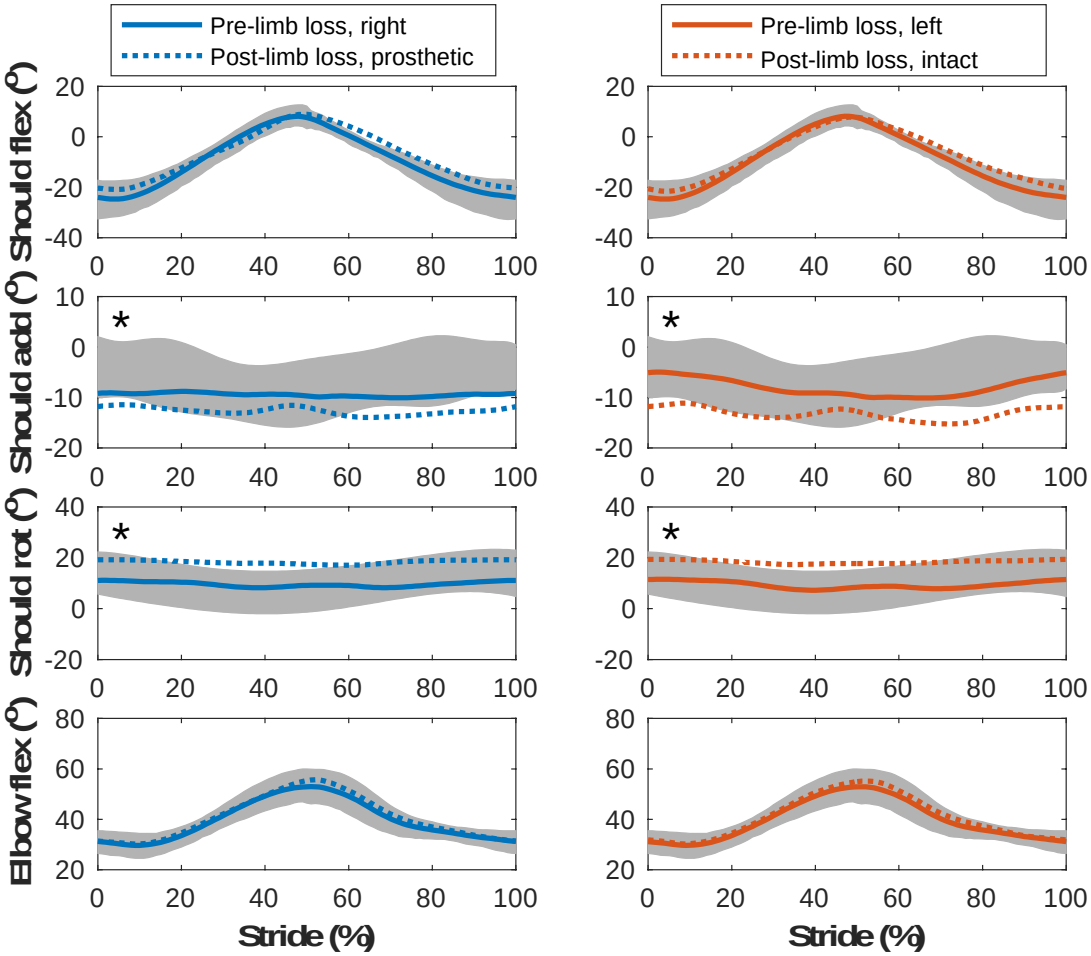

Figure 5: Upper limb joint angles during the stride cycle for the pre- limb loss (solid lines) and post-limb loss (broken lines) simulations. Data begin and end at heel-strike of the leg indicated in the column headings. Shaded areas are one standard deviation around mean human experimental walking data (Miller et al., 2014). Panels marked with * were variables with reduced tracking weight in the simulation cost function.

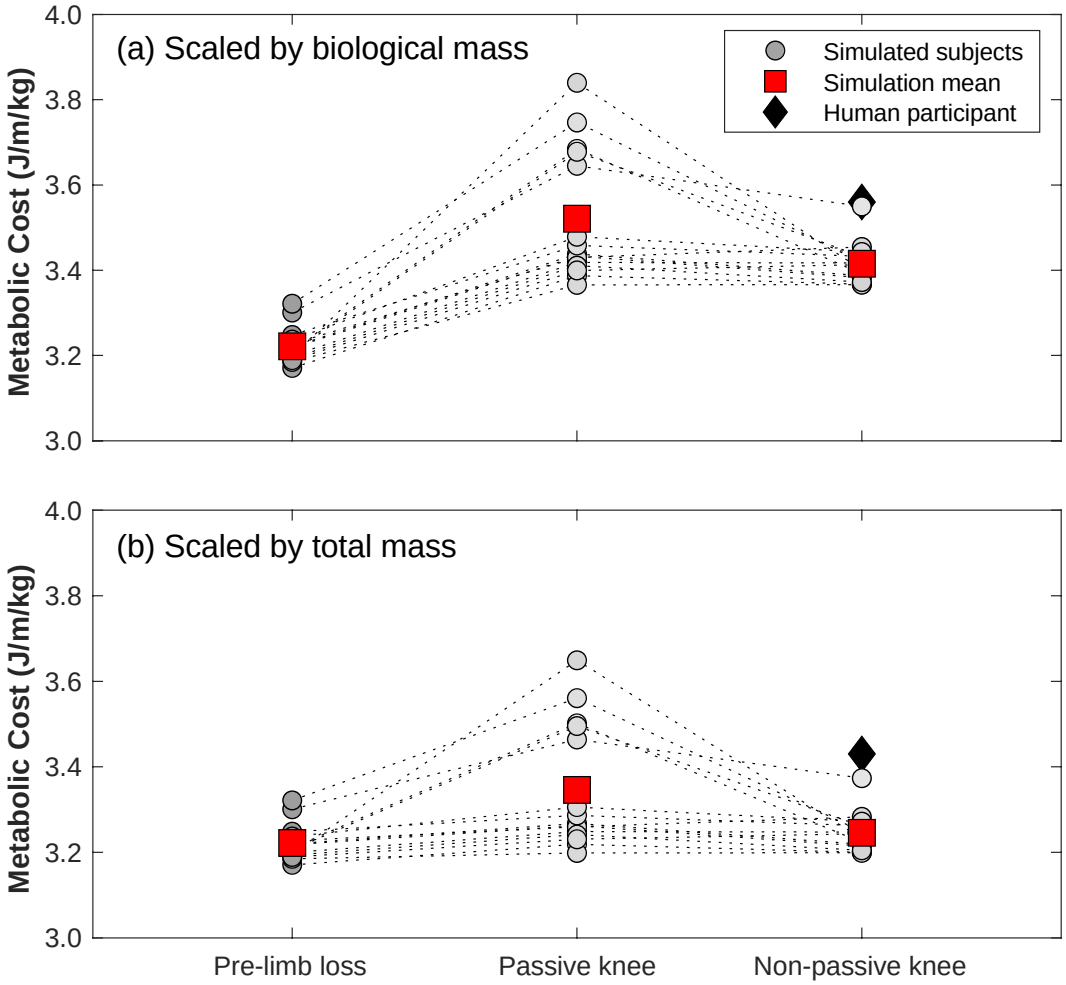

Figure 6: Gross metabolic cost of walking in simulations with the pre-limb loss model, the post-limb loss model with a passive prosthetic knee, and the post-limb loss model with a non-passive prosthetic knee. Circles are individual subject results, lines connect the same subject between conditions, and squares are mean values in each condition. Data in (a) are scaled by biological body mass, i.e. excluding the prosthesis mass. Data in (b) are scaled by total body mass, i.e. including the prosthesis mass. Diamond symbol is data from a high-functioning young adult male with unilateral transfemoral limb loss using a microprocessor-controlled prosthetic knee.